Journal of Materials Chemistry C

PAPER

Cite this: J. Mater. Chem. C, 2016, 4, 10347

Initiator-free crosslinking of oxetane functionalized low bandgap polymers: an approach towards stabilized bulk heterojunction solar cells†

Philipp Knauer,[a] Tobias Hahn,[b] Anna Köhler[bc] and Peter Strohriegl*[ac]

Received 28th July 2016,
Accepted 10th October 2016

DOI: 10.1039/c6tc03214a

www.rsc.org/MaterialsC

A critical issue of bulk heterojunction (BHJ) solar cells is the instability of the morphology of the polymer:fullerene blend over long operation times. We report the synthesis of crosslinkable derivatives of the low bandgap polymer PFDTBT, poly(2,7-(9,9-dialkylfluorene)-*alt*-(5,5-(4′,7′-di-2-thienyl-2′,1′,3′-benzothiadiazole))), and the stabilization of BHJ solar cells by crosslinking. Oxetane units are attached to the polymer side chains as crosslinkable functional groups. We study the crosslinking of the polymers *via* cationic ring opening polymerization of the oxetanes and show that our materials rapidly form insoluble networks. Our materials also crosslink in the presence of fullerenes. We report for the first time that crosslinking takes place upon prolonged heating to 100 °C without any added initiator. The best efficiency and thermal stability are found in thermally crosslinked BHJ solar cells. After 30 hours at 100 °C, 65% of the initial efficiency are retained and no further decay is observed up to 100 hours.

1. Introduction

The bulk heterojunction (BHJ) is the most popular concept for the active layer of organic solar cells based on conjugated polymers.[1] Typically, a conjugated polymer and a low-molar mass fullerene derivative, such as PCBM, are mixed together.[2] However, such a donor acceptor blend only achieves its best solar cell performance if the morphology meets certain requirements: domains in the range of the exciton diffusion length of about 10 nm ensure that excitons can reach a donor–acceptor interface within their lifetime and separate into electrons and holes.[3] Such domain sizes also result in a large donor–acceptor interface area.[4] Furthermore, an ideal morphology comprises a bicontinuous network of donor and acceptor materials.[5] This provides paths for both kinds of charge carriers towards the electrodes.

Obviously, controlling the morphology is the crucial point of the BHJ approach.[6] Different strategies to control the blend morphology during device fabrication are known: the choice of solvent,[7] solvent additives,[8,9] thermal annealing[10] or solvent vapor annealing[11] can help achieving an optimum morphology. However, this complex morphology is thermodynamically unstable and prone to macrophase separation on a long timescale.[12] This effect is even enhanced if one component tends to crystallize.[13] Once degradation of the nanoscale morphology occurs, the overall performance of an organic solar cell will drop significantly.[12]

In recent years, crosslinking emerged as an approach to freeze the morphology of a donor–acceptor blend and thus improve its long term stability.[14,15] Basically, three concepts for crosslinking bulk heterojunction materials are known: crosslinking the donor polymer,[16–20] crosslinking the acceptor,[21,22] and crosslinking the donor and the acceptor.[23] In most cases crosslinking proceeds *via* functional groups attached to the side chains of the organic semiconducting materials. Bromide,[24] vinyl,[25] styryl,[20,22] acrylate,[26] azide,[27,28] and oxetane[29] are popular crosslinkable groups.

Among these, bromide and acrylate units crosslink by free radical mechanisms,[30] vinyl and styryl groups by cycloaddition or radical mechanisms, and azides *via* nitrenes.[31,32] In this work, oxetane was chosen as the crosslinkable moiety. In this case crosslinking takes place by a cationic ring-opening polymerization (CROP).[33] The cationic mechanism is suitable for crosslinking in the presence of strongly electron accepting fullerene derivatives.

In the past we have worked on the crosslinking of polyfluorenes with acrylate groups.[34] Recently, we have reported that the diffusion of C_{60} in polyfluorene can be slowed down by a factor of 1000 by crosslinking.[35] Here, we extended our work to crosslinkable donor acceptor type polymers and chose PFDTBT,

[a] Macromolecular Chemistry I, University of Bayreuth, 95440 Bayreuth, Germany. E-mail: peter.strohriegl@uni-bayreuth.de
[b] Experimental Physics II, University of Bayreuth, 95440 Bayreuth, Germany
[c] Bayreuth Institute of Macromolecular Science (BIMF), University of Bayreuth, 95440 Bayreuth, Germany

† Electronic supplementary information (ESI) available. See DOI: 10.1039/c6tc03214a

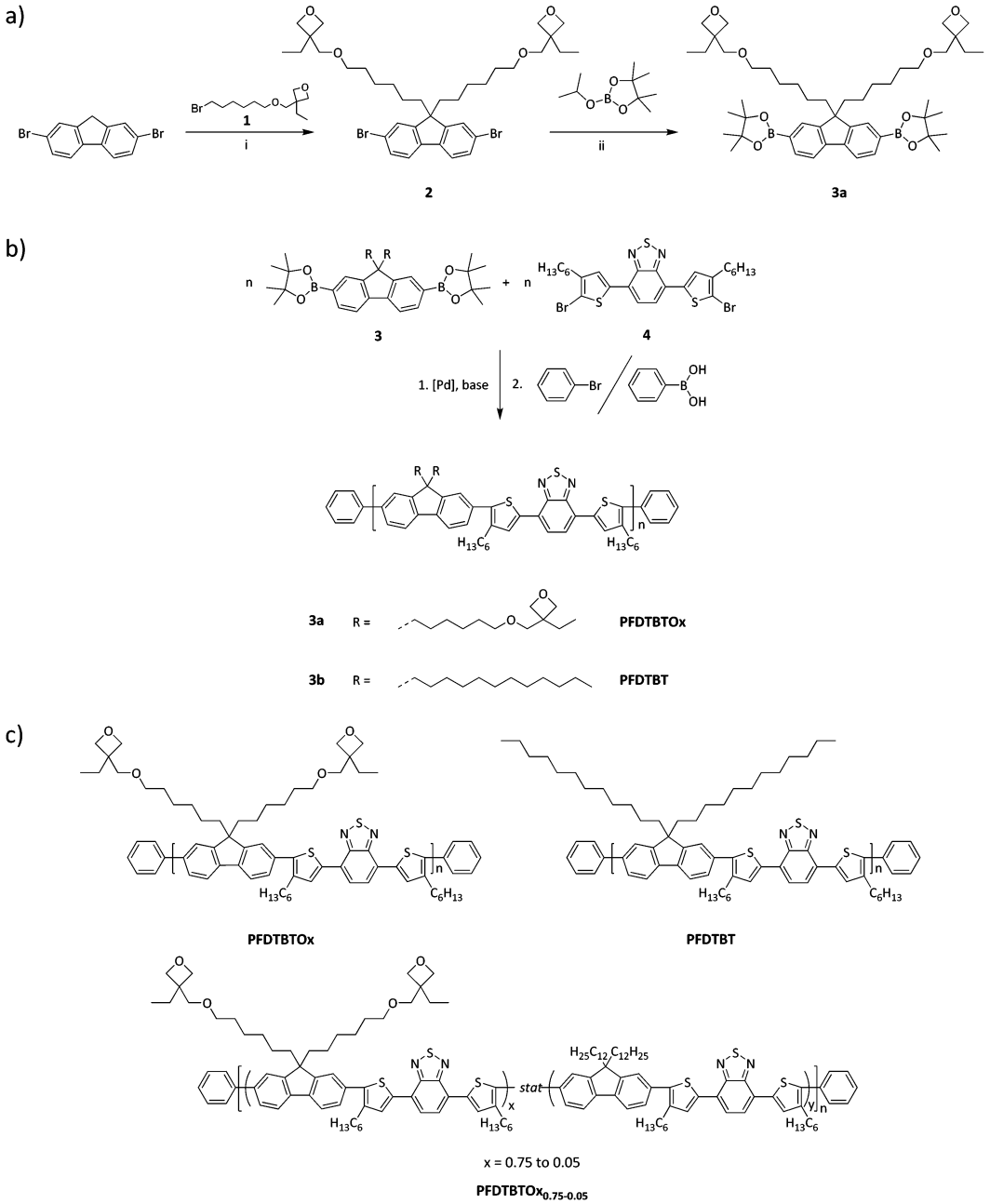

Fig. 1 (a) Synthesis of the crosslinkable fluorene monomer. Conditions: (i): DMSO, 50% NaOH, phase-transfer catalysts benzyltriethylammonium chloride and tetrabutylammonium chloride, 100 °C; (ii) THF, *n*-butyllithium, −78 °C. (b) Suzuki polycondensation. Conditions: toluene:water, $Pd(PPh_3)_4$, Na_2CO_3, aliquat 336, reflux, 4 d. (c) Chemical structures of the crosslinkable PFDTBTOx, the non-crosslinkable reference polymer PFDTBT and copolymers with different amounts of crosslinkable groups.

poly(2,7-(9,9-dialkylfluorene)-*alt*-(5,5-(4′,7′-di-2-thienyl-2′,1′,3′-benzothiadiazole))), which has been used in organic solar cells.[36] The structure is modified with solubilizing side chains at the thiophene rings and with crosslinkable oxetane units attached to the side chains of the fluorene moiety (Fig. 1b). A series of polymers with different amounts of oxetane is synthesized and the crosslinking efficiency is assessed both for crosslinking upon exposure to trifluoroacetic acid (TFA) at 80 °C and for initiator-free crosslinking upon heating to 100 °C. The polymer with the highest number of oxetane groups is tested in BHJ solar cells. In particular the thermal stability during annealing at 100 °C for up to 100 hours is investigated.

2. Results and discussion

2.1 Synthesis

The synthetic steps towards the crosslinkable fluorene monomer are shown in Fig. 1a. 3-(6-Bromohexyloxymethyl)-3-ethyloxetane **1** was synthesized from 3-ethyloxetanemethanol and

1,6-dibromohexane.[37] In a biphasic mixture of DMSO and NaOH, 2,7-dibromofluorene was deprotonated at the C-9 position and substituted with two oxetane chains to yield the fluorene derivative **2**. The crosslinkable fluorene monomer **3a** is obtained after reacting **2** with isopropoxyboronic acid pinacol ester. The purity of **3a** is crucial for the ensuing Suzuki polycondensation. Highly pure monomers were achieved by medium pressure liquid chromatography (MPLC). The second monomer, 4,7-bis(5-bromo-4-hexyl-2-thienyl)-2,1,3-benzothiadiazole, **4** was commercially available. Suzuki polycondensation of equimolar amounts of **3** and **4** was performed in a biphasic mixture of toluene and water with $Pd(PPh_3)_4$ as a catalyst. The polymer synthesis is shown in Fig. 1b. Following workup, the polymer was purified by Soxhlet extraction with a sequence of solvents, acetone, hexane, and toluene. Due to the side chains at the thiophenes the polymer is highly soluble. For the experiments in this work, the hexane fractions were used.

As a reference material a non-crosslinkable PFDTBT with dodecyl chains at the fluorene unit was synthesized by the same procedure. The chemical structures of both materials are shown in Fig. 1c. From size exclusion chromatography (SEC) (Fig. 2a) the molecular weights of the polymers were determined. The molecular weights of PFDTBTOx ($\overline{M_n}$ 14 800 g mol^{-1}, $\overline{M_w}$ 37 900 g mol^{-1}) and the reference PFDTBT ($\overline{M_n}$ 11 500 g mol^{-1}, $\overline{M_w}$ 24 000 g mol^{-1}) are within the same range. UV-Vis absorption and photoluminescence spectra of PFDTBTOx and PFDTBT are almost identical. Only a small red-shift is visible in the photoluminescence spectrum of PFDTBTOx (Fig. 2b). Both materials are thermally stable up to 400 °C in an inert atmosphere.

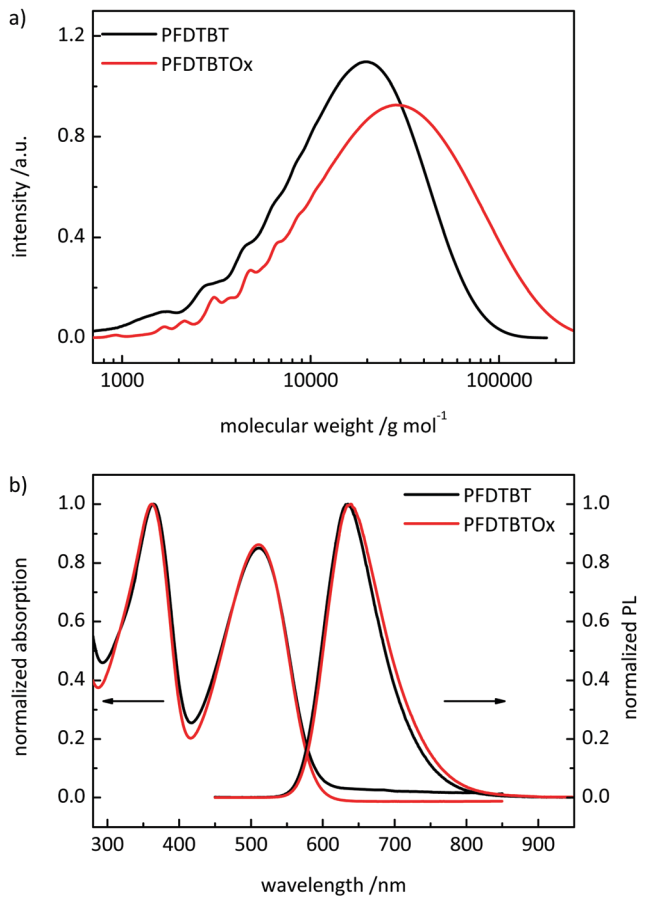

Fig. 2 Characterization of the crosslinkable low bandgap polymer PFDTBTOx and the reference polymer PFDTBT. (a) SEC traces. Eluent: THF, polystyrene calibration. (b) Absorption and photoluminescence (PL) spectra from THF solutions (c = 10^{-3} mg ml^{-1}).

Table 1 A series of low bandgap polymers with varying amounts of crosslinkable oxetane groups. The index x represents the crosslinkable fluorene monomer, and the index y represents the non-crosslinkable didodecylfluorene monomer

	Feed ratio		Found in polymers[a]		Molecular weight[b]	
	3a	3b	x	y	$\overline{M_n}$ [g mol^{-1}]	$\overline{M_w}$ [g mol^{-1}]
PFDTBTOx	1	0	1	0	14 800	37 900
PFDTBTOx$_{0.75}$	0.75	0.25	0.76	0.24	14 200	33 400
PFDTBTOx$_{0.50}$	0.50	0.50	0.52	0.48	6200	13 200
PFDTBTOx$_{0.25}$	0.25	0.75	0.25	0.75	12 500	22 500
PFDTBTOx$_{0.10}$	0.10	0.90	0.10	0.90	11 800	24 000
PFDTBTOx$_{0.05}$	0.05	0.95	0.04	0.96	11 000	21 100
PFDTBT	0	1	0	1	11 500	24 400

[a] The amount of x and y was determined from ^{1}H NMR spectra based on the integrals of the singlet at 3.45 ppm and the multiplet between 7.30 and 8.15 ppm. (For NMR data refer the experimental part.) [b] Determined from SEC, eluent: THF, $\overline{M_n}$ and $\overline{M_w}$ were calculated from polystyrene calibration.

By the same procedure a series of polymers with varying amounts of crosslinkable groups was synthesized by copolymerization of the oxetane functionalized fluorene monomer **3a** and the non-functionalized fluorene monomer **3b** with **4**. The structure of these polymers is shown in Fig. 1c. Table 1 lists the monomer feed ratios and the molecular weights of the polymers from this work.

The molecular weights of the polymers from this series are within the same range, except for PFDTBTOx$_{0.50}$ which has a lower molecular weight. From ^{1}H NMR spectra the amount of oxetane containing fluorene units in the polymers is calculated. In all the cases the amount of oxetane containing fluorene units found in the copolymers is very close to the number expected from the feed ratios.

2.2 Crosslinking

The crosslinking process of PFDTBTOx was carefully investigated. Solubility tests were performed as a measure for the success of the crosslinking reaction. This experiment compares the optical density of PFDTBTOx films before and after crosslinking and after rinsing with solvent. Film retention of 100% indicates that every polymer chain of the sample has become a part of an insoluble network.

Typically, photoacid generators (PAGs) provide protons for the initiation of the CROP of oxetanes.[38] A schematic representation of the formation of polyethers by ring-opening polymerization of oxetanes is shown in the ESI† (Fig. S1).[39] Following the activation of the PAGs by UV irradiation, the actual crosslinking reactions take place during a curing step at elevated temperature. Insoluble films of PFDTBTOx were achieved using 5 wt% of diphenyliodonium perfluorobutyl sulfonate. With 1 wt%

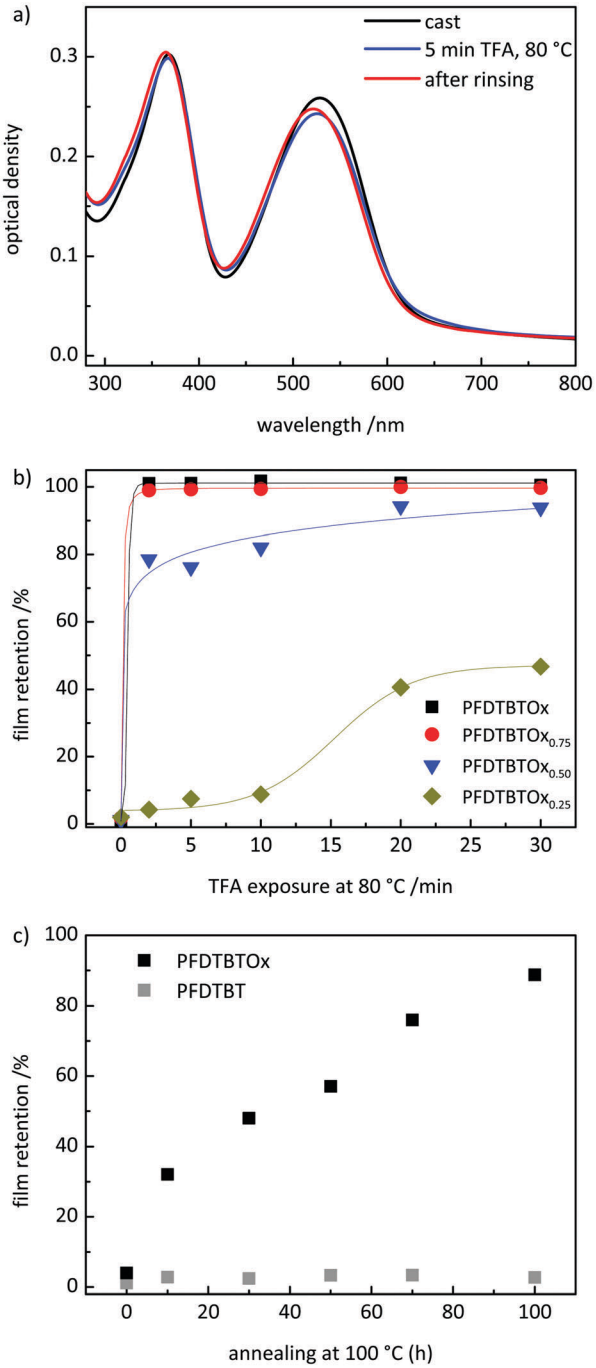

Fig. 3 Crosslinking initiated by TFA vapor (a and b) and by thermal crosslinking (c). (a) Absorption spectra of 80 nm thick films of PFDTBTOx as cast, after 5 minutes of exposure to TFA vapour at 80 °C, and after subsequently being rinsed in toluene. Insoluble films of PFDTBTOx are achieved after exposure to TFA vapor at 80 °C for five minutes. (b) Kinetics of crosslinking from solubility tests. Film retention was calculated from the optical density of films before and after rinsing with THF. Lines are only guides to the eye. (c) Kinetics of thermal crosslinking from solubility tests for annealing times up to 100 h.

PAGs only partially insoluble films were formed even after curing at 150 °C.

A very efficient initiator for the CROP is trifluoroacetic acid (TFA).[17] This strategy combines a number of advantages compared to PAGs: the samples are prepared from plain polymer solutions without any photolabile component, which needs to be taken care of during processing. The low boiling point of 78 °C and the high vapor pressure of TFA help saturating the thin sample with protons even at comparably low temperatures. This means that residual TFA can easily be removed from the films by a simple vacuum treatment. Treating PFDTBTOx with TFA vapor at 100 °C for five minutes resulted in the formation of insoluble films. The same results were achieved after reducing the temperature to 80 °C (boiling point of TFA is 78 °C). UV-Vis spectra of the corresponding solubility test are shown in Fig. 3a. After experiencing that TFA vapor rapidly leads to the formation of insoluble films of PFDTBTOx, we studied the kinetics of crosslinking in detail. Therefore, crosslinking experiments with $PFDTBTOx_{0.75}$, $PFDTBTOx_{0.50}$, and $PFDTBTOx_{0.25}$ were performed. Polymer films were exposed to TFA vapor at 80 °C for 2, 5, 10, 20, and 30 minutes. The kinetics are shown in Fig. 3b.

Polymers with high densities of oxetane groups, PFDTBTOx and $PFDTBTOx_{0.75}$, almost immediately form insoluble networks upon exposure to TFA. With $PFDTBTOx_{0.50}$ 80% film retention is achieved already after short exposure times. After 20 and 30 minutes these samples are more than 90% insoluble. The molecular weight of $PFDTBTOx_{0.50}$ is significantly lower ($\overline{M_n}$ 6800 g mol^{-1}) compared to the other polymers of this series. Consequently, it is very likely that particularly the very short polymer chains do not contain enough crosslinkable groups. In the case of such low molecular weight polymers even their formation without any crosslinkable groups cannot be ruled out. In $PFDTBTOx_{0.25}$, exposure times of 10 minutes and below do not result in any significant crosslinking; more than 90% of the films remain soluble. In this case a longer exposure time to TFA vapor helps to crosslink at least parts of the films, resulting in 50% film retention after 30 minutes. We found that our oxetane containing polymer PFDTBTOx forms partially insoluble films upon annealing for longer times, even without exposure to TFA vapor (Fig. 3c). After 10 hours at 100 °C, 30% film retention is observed. With longer annealing times the film retention is increased to more than 80% after 100 hours. This behavior is not observed for the PFDTBT reference. Consequently, we attribute this effect in PFDTBTOx to a thermally activated crosslinking of the oxetane groups which to our knowledge has not been reported earlier.

With respect to its application in BHJ solar cells the crosslinking of PFDTBTOx in blends with PCBM was investigated. As described for the neat polymer, solubility tests were conducted. Already after short exposure times (5 minutes at 80 °C) to TFA vapor an insoluble polymer network is formed. PCBM is not involved in the crosslinking reaction and is washed off during solvent rinsing. Spectra from this experiment can be found in Fig. S2 of the ESI.†

Prior to the fabrication of solar cells the thermal stability of polymer:PCBM blends was investigated. Therefore, blends of PFDTBTOx:PCBM and PFDTBT:PCBM were cast on glass slides. The films were annealed at 100 °C under an inert atmosphere for 15 minutes, 75 minutes, 8 hours, 30 hours, and 100 hours. After each step, the samples were checked for the presence of

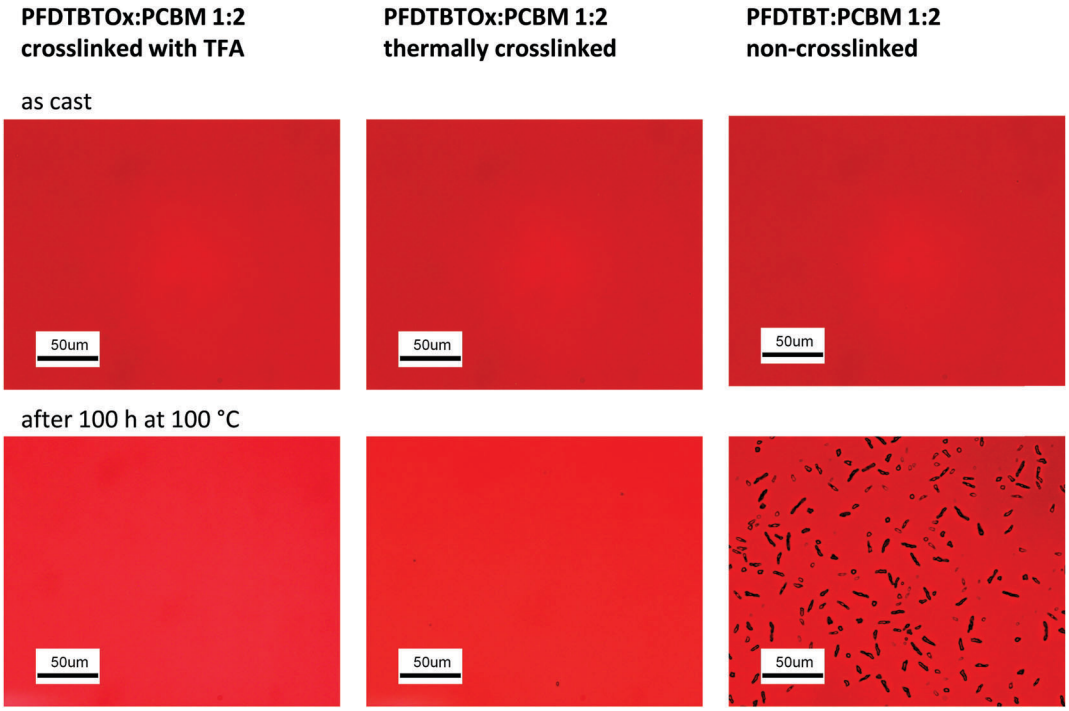

Fig. 4 Optical micrographs of polymer : PCBM 1 : 2 blends immediately after preparation and after annealing for 100 h. Crosslinked PFDTBTOx:PCBM (left column) is compared with PFDTBTOx:PCBM that was not exposed to TFA vapor (middle). The right column shows the non-crosslinkable reference PFDTBT. For enlarged pictures see Fig. S3 to S5 of the ESI.†

PCBM aggregates using polarization microscopy. We compared PFDTBTOx:PCBM blends that were crosslinked in TFA vapor prior to annealing with blends that were not exposed to TFA vapor. Furthermore, blends of the non-crosslinkable reference PFDTBT were analyzed. The micrographs of the polymer : PCBM 1 : 2 blends after annealing for 100 hours are shown in Fig. 4. Within the resolution of the optical microscope no aggregates can be observed in the initial state of the three samples. In the crosslinked blend shown in the left column, no aggregates can be observed for annealing times of up to 100 hours. For the PFDTBT:PCBM blend shown in the right column, a small number of aggregates can be seen in an optical microscope after 8 hours, with more aggregates appearing after 30 hours.

The stabilizing effect of crosslinking on the morphology of the low bandgap polymer:PCBM blend becomes evident from the micrographs. Furthermore, the initially non-crosslinked PFDTBTOx:PCBM seems to be much more stable than the PFDTBT:PCBM reference.

We attribute this stabilization to thermal crosslinking of the oxetane groups in PFDTBTOx. In solubility tests (Fig. 3c) we observed almost insoluble films of PFDTBTOx after annealing at 100 °C for 100 hours even without a cationic initiator.

2.3 Accelerated aging

To investigate the influence of crosslinking on the long-term stability of BHJ solar cells, accelerated aging tests were performed. In such an experiment a change in the device characteristics after long operation times is simulated. As described above, stabilizing the morphology is a crucial point for the long-term stability of BHJ solar cells. For a polymer:PCBM blend an initially optimized morphology is likely to deteriorate by diffusion of the low-molar mass fullerene leading to the formation of large aggregates of PCBM. However, PCBM diffusion is rather slow at room temperature. In an accelerated aging experiment, diffusion is increased by annealing the samples at elevated temperatures. Thus, the behavior of solar cells at long operation times can be simulated in a reasonable time. In this work, 100 °C was chosen as the temperature for the annealing process. This temperature is high enough to accelerate PCBM diffusion yet low enough to prevent thermal degradation of the active materials.

For the accelerated aging experiments BHJ solar cells of the crosslinked PFDTBTOx were compared with the non-crosslinked PFDTBTOx and with the reference polymer PFDTBT. We choose the polymer with two oxetane groups in each repeat unit to obtain a densely crosslinked network. The high crosslinking density is expected to clearly demonstrate the stabilizing effect. Polymer : PCBM ratios of 1 : 2 were investigated. This means that BHJ solar cells consist of 66 wt% of low molar mass PCBM in the polymer matrix. The steps of the accelerated aging experiment are illustrated in Fig. 5.

To monitor the development of the solar cell performance during annealing, current–voltage curves were recorded under an inert atmosphere after 15 minutes, 60 minutes, 8 hours, 30 hours, and 100 hours of thermal treatment at 100 °C. For each material combination four solar cells were measured. The *J–V* curves are shown in Fig. S6 of the ESI.† From the current–voltage characteristics the PCEs were calculated at every time

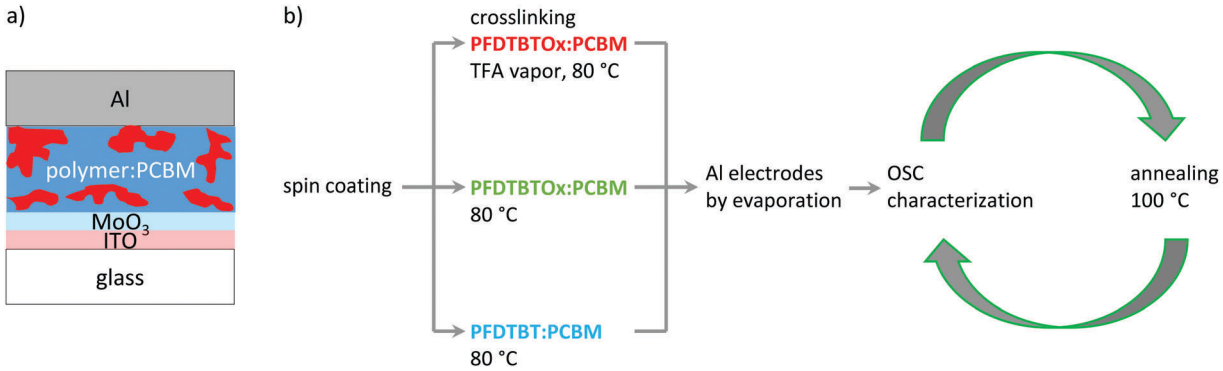

Fig. 5 Accelerated aging experiment. (a) The layer structure employed. (b) Sequence of steps for device fabrication, characterization and annealing. After spin-coating, the blends were heated to 80 °C and, in one case, the blend of PFDBTBTOx:PCBM was exposed to TFA vapor. For the second PFDTBTOx:PCBM blend and the PFDTBT:PCBM reference, TFA treatment was omitted. The aluminum electrodes were evaporated in the final step. The organic solar cells were then measured, annealed at 100 °C for a certain time, and remeasured. For all three types of organic solar cells a polymer : PCBM blend ratio of 1 : 2 was investigated.

step and the stability plots of the four individual cells are shown in Fig. S7 (ESI†).

Distinct changes are observed already at short annealing times. Thus, the development of the PCE for the first 60 minutes is discussed first (Fig. 6a and b). It can be seen that for the 1 : 2 blend of PFDTBT and PFDTBTOx the initial efficiencies are different. PFDTBT shows the highest efficiency of 0.65% followed by the non-crosslinked PFDTBTOx blend with 0.50%. We attribute this difference to the incorporation of the crosslinkable oxetane groups. We are aware of reports in the literature that the incorporation of a large number of crosslinkable groups leads to somewhat reduced initial device performance due to the disturbed packing of the chromophores.[17,40] For the crosslinked PFDTBTOx blend the initial efficiency is even lower (0.25%), yet it increases to the value of the non-crosslinked PFDTBTOx sample within 15 minutes of annealing. Looking at the development over the entire annealing time of 100 hours (Fig. 6c and d), the PCEs of the crosslinked devices reach their maxima after 15 minutes and start to decrease afterwards. The initial PCE is reached after approximately 18 hours. After 100 hours of annealing at 100 °C, the crosslinked devices retain 65% of their initial efficiency.

In the case of the thermally crosslinked PFDTBTOx devices, the most significant loss of efficiency occurs within the first eight hours of annealing. By comparison with Fig. 3c one can see that this is the time period until about one-third of the film is crosslinked. At longer times the decay is slowed down, and the PCE saturates at around 65% of the starting value. In the normalized graphs the TFA crosslinked and thermally crosslinked PFDTBTOx samples saturate at the same value for long annealing times of 100 hours.

Compared with the PFDTBTOx based devices, the solar cells comprising the PFDTBT reference polymer without crosslinkable oxetane groups behave differently. The PCE of the 1 : 2 blend device decays stepwise and no saturation is observed. Between 30 and 100 hours of annealing the most significant loss of efficiency is visible. It is noteworthy that the non-crosslinked samples, PFDTBT, show significant sample-to-sample variation, in particular within the first 40 hours. The largest variation occurs after 1 hour, when the PCE is (0.55 ± 0.10)%, *i.e.* the error is about 20% of the mean value. In contrast, the TFA crosslinked and the thermally crosslinked samples PFDTBTOx (x-linked) and PFDTBTOx, scatter significantly less around their mean value. For example, after 1 hour, a mean PCE of (0.34 ± 0.01)% is obtained for PFDTBTOx, *i.e.* the error is about 3% of the mean value. We attribute the variation in the PCE of the non-crosslinked sample to arbitrary variations in the blend morphology, *i.e.* to differences in the phase separation and percolation pathways. The reduced sample-to-sample variation in the thermally crosslinked or chemically crosslinked samples therefore seems to suggest a more reproducible blend morphology upon crosslinking.

In summary, the PCEs of PFDTBT and PFDTBTOx blends behave differently upon annealing at 100 °C. While the efficiencies of the PFDTBT reference blends decay significantly to low efficiencies, the PCEs of PFDTBTOx blends stabilize after 30 hours. For longer annealing times up to 100 hours only small changes can be observed for both PFDTBTOx samples. This behavior can be attributed to stabilization by crosslinking the polymer in the blend. Thermal crosslinking by annealing for longer times seems to be an interesting possibility to stabilize blend solar cells without reducing the efficiency by the crosslinking process itself. Fig. 6c shows that the efficiency of the initially non-crosslinked PFDTBTOx blend is higher than that of the PFDTBT blend and the same as that of the crosslinked PFDTBTOx blend after 100 hours of annealing at 100 °C.

A crosslinked polymer network can lower the diffusivity of the PCBM molecules,[35] thus preventing the aggregation of PCBM. We expect that the morphology of the crosslinked bulk heterojunctions is retained during accelerated aging, and consequently the efficiency is not further reduced.

2.4 Discussion

The accelerated aging experiments at 100 °C clearly showed that crosslinking of PFDTBTOx results in more stable BHJ solar cells. However, we experienced that the structural modification of PFDTBT by introducing oxetane groups reduces the solar cell

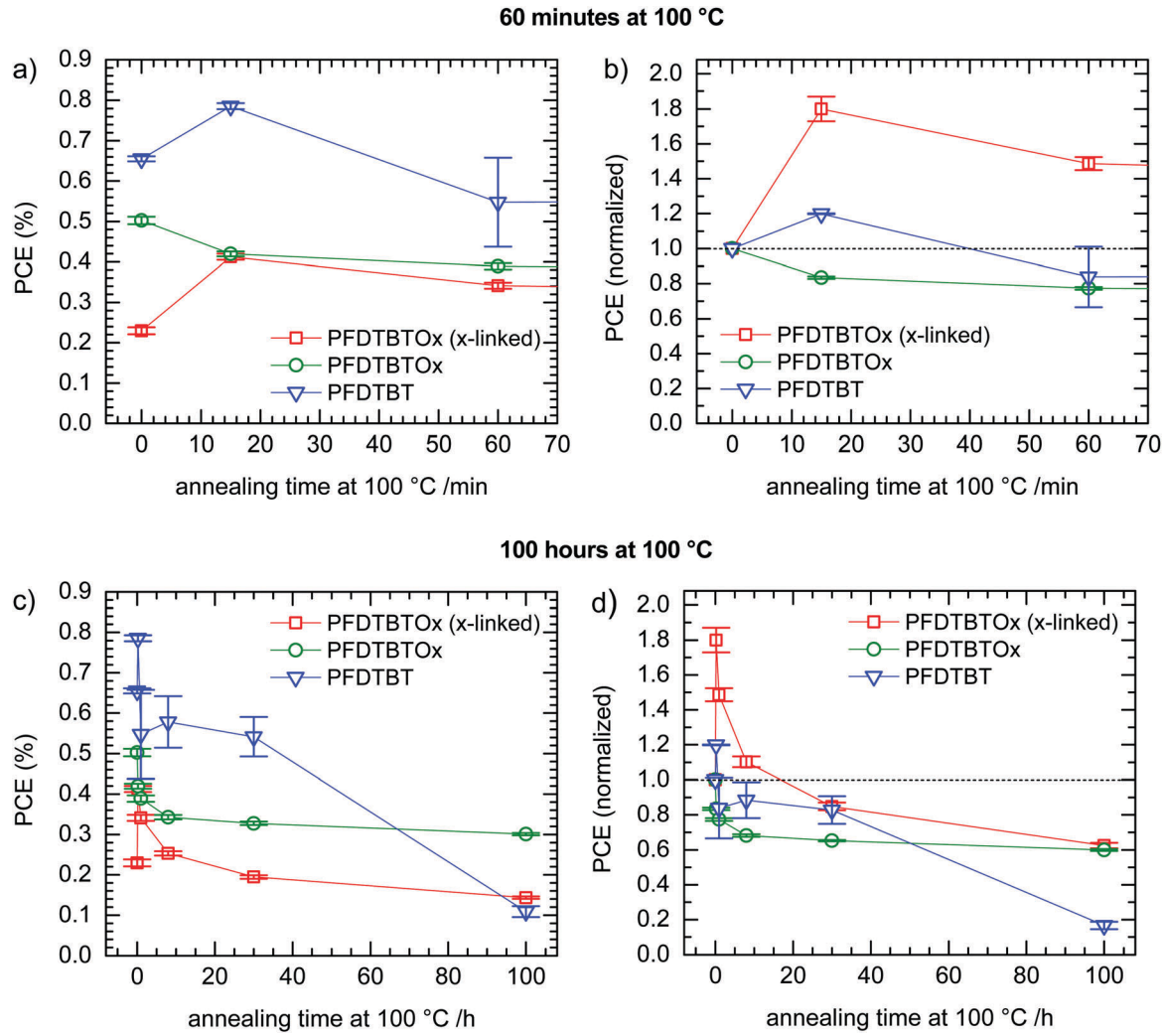

Fig. 6 Development of the PCE for the TFA crosslinked PFDTBTOx, thermally crosslinked PFDTBTOx and non-crosslinkable PFDTBT in a 1 : 2 blend ratio with PCBM. At the top the PCE during the first 60 minutes of annealing at 100 °C is displayed. At the bottom the development for up to 100 hours at 100 °C is shown. Absolute PCE values are shown on the left (a and c). On the right the relative PCE normalized to the starting value is displayed (b and d). For each system four different cells were measured. The error bars indicate the standard error obtained from four different devices, lines serve as the guide to the eye.

efficiency (ESI,† Fig. S6). This is in accordance with comparable work from the literature dealing with crosslinkable low bandgap polymers.[16,17,40] In the studies of Carlé and Yau the number of crosslinkable groups in these polymers is distinctly lower than that in PFDTBTOx. Carlé *et al.* compared different functional groups for crosslinking BHJ blends. Using a photoacid generator as an initiator for the cationic ring opening of oxetanes they crosslinked the low bandgap polymer TQ-oxetane : PCBM in 1 : 1 blends.[16] In an accelerated aging experiment at 100 °C for up to 50 hours the power conversion efficiency dropped to 50% of the initial value. Our PFDTBTOx system retains 65% of power conversion efficiency after 100 hours of annealing at 100 °C, even with a higher PCBM content (polymer : PCBM 1 : 2). We attribute this to the higher number of oxetane groups and thus a higher crosslinking density in PFDTBTOx. Yau *et al.* tested the oxetane functionalized low bandgap polymer PDTG-TPD-Ox in BHJ solar cells with $PC_{70}BM$.[17] For their stability studies they used copolymers with 0.2 oxetane groups per repeat unit. The development of the solar cell efficiency at 120 °C was monitored only in a time range of 30 minutes. We tested our devices for a much longer time period of 100 hours, which provides a more detailed insight into their long-term stability.

Importantly, we observed that the oxetane units in PFDTBTOx undergo a thermal crosslinking upon heating for a prolonged time. Among all samples investigated, the thermally crosslinked BHJ cells exhibit both the highest efficiencies and the best stability after 100 hours. This is particularly important since, in organic solar cells, an initiator-free crosslinking avoids the decomposition products of the initiator in the active layer, which might have a detrimental effect on the device performance, *e.g.* by acting as an electron trap or a quenching site.

In a recent paper Chen *et al.* investigated thermally crosslinked BHJ cells made from the donor acceptor polymer PBDTTPD with

very low amounts of crosslinkable vinyl groups.[40] For an optimized cell with 0.05 vinyl groups per repeat unit they demonstrated a stabilization process when the cells are annealed at 150 °C. Nevertheless, the solar cell efficiency still decreases after 40 hours. In contrast to this, for our thermally crosslinked PFDTBTOx cells the efficiency remains constant from 8 up to 100 hours (Fig. 6c).

Our results combined with the literature cited above demonstrate that crosslinking plays an important role in the stabilization of BHJ solar cells. In most cases crosslinkable groups are intentionally added to a given low bandgap polymer structure. In one particular case crosslinking might also be the reason for the good long-term stability observed in BHJ cells from the well-known low bandgap polymer PCDTBT.[41] Tournebize *et al.* described unintentional crosslinking in PCDTBT:PCBM blends.[30] They proposed that photoinduced cleavage of the alkyl group at the carbazole nitrogen leads to carbazolyl radicals. Subsequently, these polymer radicals undergo reactions with other polymer chains or with the electron acceptor PCBM which lead to the formation of a network.[30] This crosslinking is specific only for the carbazole containing PCDTBT. In contrast, the addition of crosslinkable groups is a more general approach, in particular as it involves the moieties on the side chain and not on the electronically active main chain, and it can be applied to all donor–acceptor type polymers.

3. Conclusion

In this work, we present the synthesis of oxetane functionalized PFDTBT low bandgap polymers termed PFDTBTOx. We show that these polymers form insoluble networks upon crosslinking. Moreover, we find that crosslinking can be obtained not only by exposure to TFA vapor at 80 °C but also thermally by heating to 100 °C without any added initiator. Initiator-free crosslinking is particularly attractive as it avoids the formation of decomposition products, and thus potential electron traps and quenching sites, from the initiator. Furthermore, we show that PFDTBTOx also crosslinks in the presence of PCBM. We demonstrate the stabilization of BHJ solar cells by crosslinking the low bandgap polymer. In accelerated aging experiments we investigated the device stability upon annealing at 100 °C for times up to 100 hours. We used blends with a ratio of 1 : 2 and followed the device performance during annealing. Stabilization was clearly observed in crosslinked BHJ cells compared to cells comprising the non-crosslinkable reference polymer. The best efficiency and thermal stability were observed for the thermally crosslinked BHJ solar cells. After 30 hours at 100 °C, almost 65% of the initial efficiency are retained and no further decay is observed up to 100 hours.

4. Experimental

Materials and methods

The starting materials were purchased from ABCR (2,7-dibromofluorene, 3-ethyl-3-oxetanemethanol), Acros Organics (Aliquat 336, benzyltriethylammonium chloride, bromobenzene, *n*-butyllithium, 2-isopropoxy-4,4,5,5-tetramethyl-1,3,2-dioxaborolane, $Pd(PPh_3)_4$), Fluka (phenylboronic acid, tetrabutylammonium chloride), Hedinger (NaOH), Carl Roth (Na_2SO_4, Na_2CO_3, tetrabutylammonium bromide), and Sigma Aldrich (1,6-dibromohexane, 1-dodecylbromide) and used as received. Dry solvents were purchased from Acros Organics. Monomer **4** (4,7-bis(5-bromo-4-hexyl-2-thienyl)-2,1,3-benzothiadiazole) was purchased from SunaTech Inc. and used without further purification.

^{1}H NMR spectra were recorded on a Bruker AC spectrometer (300 MHz) at room temperature using $CDCl_3$ as solvent. Mass spectrometry (MS) data were obtained from a FINNIGAN MAT 8500 instrument. Molecular weights were determined by size exclusion chromatography (SEC) using a Waters 515-HPLC pump with stabilized THF as the eluent at a flow rate of 0.5 ml min^{-1}. The array of columns consisted of a guard column (Varian, 50 × 0.75 cm, ResiPore particle size 3 μm) and two separation columns (Varian, 300 × 0.75 cm, ResiPore particle size 3 μm). The compounds were monitored using a Waters UV detector at 254 nm. As an internal standard 1,2-dichlorobenzene was added. Number average ($\overline{M_n}$) and weight average ($\overline{M_w}$) molecular weights were calculated based on calibration with a polystyrene standard. Thermogravimetric analysis (TGA) measurements were performed on a Mettler Toledo TGA/SDTA 851e at a heating rate of 10 K min^{-1} under nitrogen flow. UV/Vis spectra of solutions (THF, concentration 10^{-3} mg ml^{-1}) and thin films were recorded on a JASCO V-670 spectrophotometer at room temperature. Photoluminescence (PL) spectra were collected from a JASCO FP-8600 spectrofluorometer from solutions (THF, concentration 10^{-3} mg ml^{-1}) and thin films with nitrogen as purge gas. Polarized light microscopy was performed using a Nikon DIAPHOT 300 optical microscope. Optical micrographs were recorded by a Nikon ACT-1 software using a Nikon DMX1200 digital camera.

Crosslinking experiments were run using a photoacid generator (PAG) or trifluoroacetic acid (TFA) vapor as an initiator. To monitor the progress of crosslinking, solubility tests were executed. The photoacid generator DPI-109 was purchased from Midori Kagaku Co. Ltd and used without purification. Trifluoroacetic acid was purchased from Acros Organics.

For crosslinking in TFA vapor, films with a thickness of about 80 nm were prepared by spin coating on glass substrates. Polymer solutions (15 mg ml^{-1}) and solutions of polymer : PCBM (1 : 2 by weight, 30 mg ml^{-1}) in chlorobenzene were filtered through 0.20 μm Teflon filters. After spin coating, the films were dried in a vacuum at 60 °C. UV/Vis absorption spectra were recorded before crosslinking. For crosslinking, the samples were placed on a hot plate equipped with a glass cover, which was flushed with argon, and a glass dish, in which trifluoroacetic acid (2 ml) was added. Crosslinking experiments were performed at 80 °C and 100 °C for five to 60 minutes. Residual TFA was removed from the samples by storage in a vacuum for 60 minutes. Afterwards, UV/Vis absorption spectra were recorded. The films were rinsed with THF for 30 seconds and dried in air. Ultimately, UV/Vis absorption spectra were recorded.

Bulk heterojunction organic solar cell devices were fabricated on structured glass substrates coated with indium tin oxide (ITO). A circular active area (7.07 mm^2) was defined on top of the ITO

layer using a photoresist (AZ 1518, supplier: Microchemicals).[42] On the active area, a 15 nm thick layer of MoO_3 (Sigma Aldrich) was added by vacuum evaporation. The MoO_3 layer ensures a low dark current and a good diode behavior.

The active layer was applied by spin coating. From chlorobenzene solutions (20 mg ml^{-1}), 80 nm thick layers of the polymer:PCBM blends were cast. PCBM (99.5% purity, Sigma Aldrich) was used as an acceptor in the blend. PCBM and polymer solutions (20 mg ml^{-1}) were produced separately, filtered through a 0.4 μm Teflon filter and mixed in a 1 : 2 ratio. The layer thicknesses of the blends for each polymer were controlled with a Dektak (Veeco) profilometer directly on the device. Optionally, crosslinking in TFA vapor was performed in an argon glovebox at 80 °C for 20 minutes (5 minutes heating up, 15 minutes exposure to TFA vapor). The reference solar cells were annealed for the same time and temperature (20 minutes, 80 °C) in a TFA vapor free nitrogen atmosphere for comparability purposes. The devices were put under vacuum in the evaporation chamber for 10 hours at 10^{-7} mbar until the evaporation was started. We took special care to avoid contact between the TFA crosslinked samples and the other solar cells to avoid cross-contamination with TFA. Finally, a 100 nm thick aluminium cathode was vacuum evaporated.

Current–voltage characteristics under AM1.5 sunlight conditions were measured with a Newport sun simulator and an appropriate vacuum condition sample holder to prevent oxygen degradation of the device during the measurement. For solar cell measurements a Keithley 238 source-measure-unit was used.

Accelerated aging was realized by annealing the solar cells at 100 °C on a hot plate in a nitrogen glovebox. Prior to the first annealing step, the efficiencies of all devices were measured. After every annealing time step, all devices were measured again and brought back to the hot plate in the glovebox. The annealing times given in the text are total annealing times, respectively. Using the vacuum condition sample holder, an oxygen free transport of the devices from the glovebox to the sun simulator was guaranteed.

The standard error s in Fig. 6 was determined from the values x_i obtained by measuring four independently prepared samples according to $s = \sqrt{\frac{\sum (x_i - \bar{x})^2}{n(n-1)}}$.

Synthesis

3-(6-Bromohexyloxymethyl)-3-ethyloxetane 1. The reactants 3-ethyl-3-oxetanemethanol (5.81 g, 50.00 mmol) and 1,6-dibromohexane (36.60 g, 150.00 mmol), and the phase-transfer catalyst tetrabutylammonium bromide (0.80 g, 2.50 mmol) were dissolved in hexane (200 ml). After the addition of a 45% NaOH (28 ml), the mixture was heated to reflux for 16 hours. The solution was poured into ice water and extracted with hexane. The combined hexane phases were washed with water and dried over magnesium sulfate. Following the removal of the solvent, the crude product was purified by column chromatography (gradient hexane → THF). Excess 1,6-dibromohexane was eluted with hexane before the product was eluted with THF. The solvent was removed, and 3-(6-bromohexyloxymethyl)-3-ethyloxetane (11.13 g, 39.86 mmol, 80%) was obtained as a colorless liquid. EI-MS (*m*/*z*, %): calculated for $C_{12}H_{23}BrO_2$ 279.21; found 248 (M^+ $-C_2H_5$, 40%). ^{1}H NMR (300 MHz, $CDCl_3$, δ in ppm): 0.86 (t, J = 7.5 Hz, 3H, $-CH_3$), 1.32–1.50 (m, 4H, $-CH_2-$), 1.58 (qui, J = 6.6 Hz, 2H, $-\underline{CH_2}-CH_2-O$), 1.72 (q, J = 7.5 Hz, 2H, $-\underline{CH_2}-CH_3$), 1.85 (qui, J = 6.6 Hz, 2H, $Br-CH_2-\underline{CH_2}-$), 3.36–3.47 (m, 4H, $Br-\underline{CH_2}-\cdots-\underline{CH_2}-O$), 3.51 (s, 2H, $-O-CH_2-$oxetane), 4.36, 4.43 (2d, J = 5.8 Hz, 2 × 2H oxetane CH_2).

2,7-Dibromo-9,9-bis(hexyl-6,1-diyl)bis(oxymethyl-3-ethyloxetane)-fluorene 2. A solution of 2,7-dibromofluorene (2.00 g, 6.17 mmol) and the phase-transfer catalysts benzyltriethylammonium chloride (0.06 g, 0.35 mmol) and tetrabutylammonium chloride (0.07 g, 0.35 mmol) in DMSO (45 ml) was flushed with argon for 30 minutes. Under argon 20 ml of 50% NaOH solution were added dropwise. After stirring for 20 minutes, 3-(6-bromohexyloxymethyl)-3-ethyloxetane (5.24 g, 18.51 mmol) was added dropwise. The mixture was heated to reflux for 20 hours. After cooling to room temperature, the solution was poured into ice water and extracted with diethyl ether. The combined ether phases were washed with water and dried over sodium sulfate. The solvent was removed, and the crude product was purified by flash chromatography (eluent hexane/ethyl acetate 3 : 1) yielding 2,7-dibromo-9,9-bis(hexyl-6,1-diyl)bis(oxymethyl-3-ethyloxetane)-fluorene (3.10 g, 4.30 mmol, 70%) as a yellowish oil. EI-MS (*m*/*z*, %): calculated for $C_{37}H_{52}Br_2O_4$ 720.61; found 720 (M^+, 100%). ^{1}H NMR (300 MHz, $CDCl_3$, δ in ppm): 0.48–0.64 (bs, 4H, Ar-$CH_2-\underline{CH_2}-$), 0.84 (t, J = 7.5 Hz, $-CH_3$), 1.00–1.16 (m, 8H, $-CH_2-$), 1.32–1.45 (m, 4H, $-CH_2-$), 1.70 (q, J = 7.5 Hz, 2H, $-\underline{CH_2}-CH_3$), 1.87–1.96 (m, 4H, Ar-CH_2-), 3.33 (t, J = 6.5 Hz, 4H, $-CH_2-O-$), 3.46 (s, 4H, $-O-\underline{CH_2}-$oxetane), 4.35, 4.41 (2d, J = 5.8 Hz, 2 × 4H, oxetane CH_2), 7.41–7.56 (m, 6H, Ar-H).

2,7-Bis(4,4,5,5-tetramethyl-1,3,2-dioxaborolane)-9,9-bis(hexyl-6,1-diyl)bis-(oxymethyl-3-ethyloxetane)-fluorene 3. A solution of 2,7-dibromo-9,9-bis(hexyl-6,1-diyl)bis(oxymethyl-3-ethyloxetane)-fluorene (0.98 g, 1.36 mmol) in dry THF (30 ml) was cooled to −78 °C. At −78 °C *n*-butyllithium (1.6 M solution in hexane, 1.87 ml, 2.99 mmol) was added slowly. The solution was stirred at −78 °C for 30 minutes before 2-isopropoxy-4,4,5,5-tetramethyl-1,3,2-dioxaborolane (0.61 g, 3.26 mmol) was added slowly. The reaction mixture was kept at −78 °C for another hour and was allowed to warm to room temperature overnight. It was poured into ice water and extracted with diethyl ether. The combined ether phases were washed with a saturated NaCl solution and dried over magnesium sulfate. The solvent was removed, and the crude product was purified by MPLC (eluent hexane/ethyl acetate 3 : 2) yielding 2,7-bis(4,4,5,5-tetramethyl-1,3,2-dioxaborolane)-9,9-bis(hexyl-6,1-diyl)bis(oxymethyl-3-ethyloxetane)-fluorene (0.63 g, 0.78 mmol, 57%) as a colorless solid. EI-MS (*m*/*z*, %): calculated for $C_{49}H_{76}B_2O_8$ 814.74; found 814 (M^+, 100%). ^{1}H NMR (300 MHz, $CDCl_3$, δ in ppm): 0.46–0.62 (bs, 4H, Ar-$CH_2-\underline{CH_2}-$), 0.83 (t, J = 7.5 Hz, 6H, oxetane-$CH_2-\underline{CH_3}$), 0.98–1.10 (m, 8H, $-CH_2-$), 1.30–1.39 (m, 4H, $-\underline{CH_2}-CH_2-O$), 1.39 (s, 24H, $-CH_3$), 1.68 (q, J = 7.5 Hz, 4H, oxetane-$\underline{CH_2}-CH_3$), 1.94–2.05 (m, 4H,

Ar-CH_2–), 3.29 (t, J = 6.6 Hz, 4H, –CH_2–O–), 3.44 (s, 4H, –O–$\underline{CH_2}$–oxetane), 4.38, 4.33 (2d, J = 5,8 Hz, 2 × 4H, oxetane CH_2), 7.70–7.83 (m, 6H, Ar-H).

Poly(2,7-(9,9-bis(hexyl-6,1-diyl)bis(oxymethyl-3-ethyloxetane)-fluorene)-*alt*-(5,5-(4′,7′-bis(4-hexylthien-2-yl)-2′,1′,3′-benzothiadiazole))) PFDTBTOx:. Equimolar amounts of the monomers 2,7-bis(4,4,5,5-tetramethyl-1,3,2-dioxaborolane)-9,9-bis(hexyl-6,1-diyl)bis(oxymethyl-3-ethyloxetane)-fluorene (241.00 mg, 0.296 mmol) and 4,7-bis(5-bromo-4-hexyl-2-thienyl)-2,1,3-benzothiadiazole (185.00 mg, 0.296 mmol) were dissolved in toluene (10 ml). A few drops of the phase-transfer catalyst Aliquat 336 and a 2 M solution of Na_2CO_3 (12 ml) were added, and the mixture was degassed by three freeze–pump–thaw cycles. After addition of the catalyst $Pd(PPh_3)_4$ (0.015 eq., 5.00 mg, 4.44×10^{-3} mmol) another freeze–pump–thaw cycle was applied. The reaction mixture was heated to reflux under vigorous stirring. After four days, bromobenzene and phenylboronic acid (0.296 mmol each) were added to endcap the polymer. The organic phase was separated, concentrated, and precipitated from methanol. The dried product was collected, dried, re-dissolved and precipitated from methanol, again. After drying, 210 mg (0.204 mmol, 71%) of the crude polymer were obtained. Soxhlet extraction with the sequence acetone, hexane and toluene was applied, and the fractions were concentrated and precipitated from methanol. For the experiments in this work the hexane fraction was used. ^{1}H NMR (300 MHz, $CDCL_3$, δ in ppm): 0.54–0.94 (m, 16H, –CH_3 + fluorene–CH_2–$\underline{CH_2}$–), 1.10–1.85 (m, 38H, –CH_2–), 1.92–2.20 (m, 4H, fluorene–CH_2–), 2.66–2.93 (m, 4H, thiophene–CH_2–), 3.34 (t, J = 6.5 Hz, 4H, –CH_2–O–), 3.44 (s, 4H, –O–CH_2–oxetane), 4.32 + 4.39 (2d, J = 5.7 Hz, 2 × 4H, oxetane $\underline{CH_2}$), 7.30–8.15 (m, 10H, Ar-H). SEC (THF, PS calibration): $\overline{M_n}$ 14 800 g mol^{-1}, $\overline{M_w}$ 37 900 g mol^{-1}, D 2.56. UV/Vis absorption (THF, 10^{-3} mg ml^{-1}): λ_{max}: 362 nm, 510 nm. TGA (10 K min^{-1}, N_2): 5% weight loss at 410 °C.

Poly(2,7-(9,9-didodecylfluorene)-*alt*-(5,5-(4′,7′-bis(4-hexylthien-2-yl)-2′,1′,3′-benzothia-diazole))) PFDTBT. The polymerization was performed analogous to PFDTBTOx with the monomers 2,7-bis(4,4,5,5-tetramethyl-1,3,2-dioxaborolane)-9,9-didodecylfluorene (233.37 mg, 0.309 mmol) and 4,7-bis(5-bromo-4-hexyl-2-thienyl)-2,1,3-benzothiadiazole (193.60 mg, 0.309 mmol). After work up, 265 mg (0.273 mmol, 88%) of the crude polymer were obtained. Soxhlet extraction with the sequence acetone, hexane and toluene was applied, and the fractions were concentrated and precipitated from methanol. For the experiments in this work the hexane fraction was used. ^{1}H NMR (300 MHz, $CDCl_3$, δ in ppm): 0.58–0.96 (m, 16H, –CH_3 + fluorene–CH_2–$\underline{CH_2}$–), 1.00–1.48 (m, 45H, –CH_2–), 1.66–1.85 (m, 4H, thiophene–CH_2–$\underline{CH_2}$–), 1.91–2.20 (m, 4H, fluorene–CH_2–), 2.67–2.93 (m, 4H, thiophene–CH_2–), 7.46–8.11 (m, 10H, Ar-H). SEC (THF, PS calibration): hexane fraction: $\overline{M_n}$ 11 500 g mol^{-1}, $\overline{M_w}$ 24 400 g mol^{-1}, D 2.11. UV/Vis absorption (THF, 10^{-3} mg ml^{-1}): λ_{max}: 365 nm, 511 nm. TGA (10 K min^{-1}, N_2): 5% weight loss at 420 °C.

As an example for the copolymers, $PFDTBTOx_{0.75}$ is described. The other polymers are synthesized in an analogous fashion. The monomers 2,7-bis(4,4,5,5-tetramethyl-1,3,2-dioxaborolane)-9,9-bis(hexyl-6,1-diyl)bis(oxymethyl-3-ethyloxetane)-fluorene (190.09 mg, 0.233 mmol), 2,7-bis(4,4,5,5-tetramethyl-1,3,2-dioxaborolane)-9,9-didodecylfluorene (58.87 mg, 0.078 mmol) and 4,7-bis(5-bromo-4-hexyl-2-thienyl)-2,1,3-benzothiadiazole (195.48 mg, 0.312 mmol) were dissolved in toluene (10 ml). The further procedure was the same as that for PFDTBTOx. After drying, 274 mg (0.271 mmol, 87%) of $PFDTBTOx_{0.75}$ were obtained. ^{1}H NMR (300 MHz, $CDCL_3$, δ in ppm): 0.62–0.96 (m, 16H, –CH_3 + fluorene–CH_2–$\underline{CH_2}$–), 1.02–1.50 (m, 31H, –CH_2–), 1.62–1.85 (m, 7H, thiophene–CH_2–$\underline{CH_2}$– + oxetane–$\underline{CH_2}$–CH_3), 1.92–2.21 (m, 4H, fluorene–CH_2–), 2.67–2.91 (m, 4H, thiophene–CH_2–), 3.34 (t, J = 6.6 Hz, 3H, –CH_2–O–), 3.45 (s, 3H, –O–CH_2–oxetane), 4.32 + 4.39 (2d, J = 5.8 Hz, 2 × 3H, oxetane CH_2), 7.50–8.10 (m, 10H, Ar-H). Polymer SEC (THF, PS calibration): $\overline{M_n}$ 14 200 g mol^{-1}, $\overline{M_w}$ 33 400 g mol^{-1}, D 2.35. UV/Vis absorption (THF, 10^{-3} mg ml^{-1}): λ_{max}: 365 nm, 510 nm, λ_{onset}: 584 nm, $E_{opt} \approx$ 2.10 eV. PL (THF, 10^{-3} mg ml^{-1}): λ_{max}: 634 nm. TGA (10 K min^{-1}, N_2): 1% weight loss at 368 °C, 5% weight loss at 426 °C.

Acknowledgements

We thank Irene Bauer and Frank Schirmer for technical assistance and Frank-Julian Kahle and Steffen Tscheuschner for stimulating discussions. Financial support from the Bavarian State Ministry of Science, Research, and the Arts through the Collaborative Research Network "Solar Technologies go Hybrid" and from the German Science Foundation DFG through the doctoral training center "GRK 1640" is acknowledged.

References

1 A. J. Heeger, *Adv. Mater.*, 2014, **26**, 10.
2 G. Yu, J. Gao, J. C. Hummelen, F. Wudl and A. J. Heeger, *Science*, 1995, **270**, 1789.
3 M. C. Scharber and N. S. Sariciftci, *Prog. Polym. Sci.*, 2013, **38**, 1929.
4 L. Lu, T. Zheng, Q. Wu, A. M. Schneider, D. Zhao and L. Yu, *Chem. Rev.*, 2015, **115**, 12666.
5 T. Wang, A. J. Pearson and D. G. Lidzey, *J. Mater. Chem. C*, 2013, **1**, 7266.
6 C. J. Brabec, N. S. Sariciftci and J. C. Hummelen, *Adv. Funct. Mater.*, 2001, **11**, 15.
7 S. H. Park, A. Roy, S. Beaupré, S. Cho, N. Coates, J. S. Moon, D. Moses, M. Leclerc, K. Lee and A. J. Heeger, *Nat. Photonics*, 2009, **3**, 297.
8 J. Peet, M. L. Senatore, A. J. Heeger and G. C. Bazan, *Adv. Mater.*, 2009, **21**, 1521.
9 J. K. Lee, W. L. Ma, C. J. Brabec, J. Yuen, J. S. Moon, J. Y. Kim, K. Lee, G. C. Bazan and A. J. Heeger, *J. Am. Chem. Soc.*, 2008, **130**, 3619.
10 F. Padinger, R. S. Rittberger and N. S. Sariciftci, *Adv. Funct. Mater.*, 2003, **13**, 85.
11 V. D. Mihailetchi, H. Xie, B. de Boer, L. M. Popescu, J. C. Hummelen, P. W. M. Blom and L. J. A. Koster, *Appl. Phys. Lett.*, 2006, **89**, 12107.

12 M. Jørgensen, K. Norrman, S. A. Gevorgyan, T. Tromholt, B. Andreasen and F. C. Krebs, *Adv. Mater.*, 2012, **24**, 580.
13 A. R. Campbell, J. M. Hodgkiss, S. Westenhoff, I. A. Howard, R. A. Marsh, C. R. McNeill, R. H. Friend and N. C. Greenham, *Nano Lett.*, 2008, **8**, 3942.
14 G. Wantz, L. Derue, O. Dautel, A. Rivaton, P. Hudhomme and C. Dagron-Lartigau, *Polym. Int.*, 2014, **63**, 1346.
15 J. W. Rumer and I. McCulloch, *Mater. Today*, 2015, **18**, 425.
16 J. E. Carlé, B. Andreasen, T. Tromholt, M. V. Madsen, K. Norrman, M. Jørgensen and F. C. Krebs, *J. Mater. Chem.*, 2012, **22**, 24417.
17 C. P. Yau, S. Wang, N. D. Treat, Z. Fei, B. J. Tremolet de Villers, M. L. Chabinyc and M. Heeney, *Adv. Energy Mater.*, 2015, **5**, 1401228.
18 G. Brotas, J. Farinhas, Q. Ferreira, R. Rodrigues, I. L. Martins, J. Morgado and A. Charas, *J. Polym. Sci., Part A: Polym. Chem.*, 2014, **52**, 652.
19 G. Griffini, J. D. Douglas, C. Piliego, T. W. Holcombe, S. Turri, J. M. J. Fréchet and J. L. Mynar, *Adv. Mater.*, 2011, **23**, 1660.
20 H. Waters, J. Kettle, S.-W. Chang, C.-J. Su, W.-R. Wu, U.-S. Jeng, Y.-C. Tsai and M. Horie, *J. Mater. Chem. A*, 2013, **1**, 7370.
21 C.-Z. Li, H.-L. Yip and A. K.-Y. Jen, *J. Mater. Chem.*, 2012, **22**, 4161.
22 Y.-J. Cheng, C.-H. Hsieh, P.-J. Li and C.-S. Hsu, *Adv. Funct. Mater.*, 2011, **21**, 1723.
23 M. S. Ryu and J. Jang, *Sol. Energy Mater. Sol. Cells*, 2010, **94**, 1384.
24 B. J. Kim, Y. Miyamoto, B. Ma and J. M. J. Fréchet, *Adv. Funct. Mater.*, 2009, **19**, 2273.
25 U. R. Lee, T. W. Lee, M. H. Hoang, N. S. Kang, J. W. Yu, K. H. Kim, K.-G. Lim, T.-W. Lee, J.-I. Jin and D. H. Choi, *Org. Electron.*, 2011, **12**, 269.
26 R. Penterman, S. I. Klink, H. de Koning, G. Nisato and D. J. Broer, *Nature*, 2002, **417**, 55.
27 B. Gholamkhass and S. Holdcroft, *Chem. Mater.*, 2010, **22**, 5371.
28 Z.-K. Tan, K. Johnson, Y. Vaynzof, A. A. Bakulin, L.-L. Chua, P. K. H. Ho and R. H. Friend, *Adv. Mater.*, 2013, **25**, 4131.
29 C. D. Müller, A. Falcou, N. Reckefuss, M. Rojahn, V. Wiederhirn, P. Rudati, H. Frohne, O. Nuyken, H. Becker and K. Meerholz, *Nature*, 2003, **421**, 829.
30 A. Tournebize, A. Rivaton, J.-L. Gardette, C. Lombard, B. Pépin-Donat, S. Beaupré and M. Leclerc, *Adv. Energy Mater.*, 2014, **4**, 1301530.
31 H. J. Kim, A.-R. Han, C.-H. Cho, H. Kang, H.-H. Cho, M. Y. Lee, J. M. J. Fréchet, J. H. Oh and B. J. Kim, *Chem. Mater.*, 2012, **24**, 215.
32 L. Derue, O. Dautel, A. Tournebize, M. Drees, H. Pan, S. Berthumeyrie, B. Pavageau, E. Cloutet, S. Chambon and L. Hirsch, *et al.*, *Adv. Mater.*, 2014, **26**, 5831.
33 S. Feser and K. Meerholz, *Chem. Mater.*, 2011, **23**, 5001.
34 E. Scheler and P. Strohriegl, *J. Mater. Chem.*, 2009, **19**, 3207.
35 F. Fischer, T. Hahn, H. Bässler, I. Bauer, P. Strohriegl and A. Köhler, *Adv. Funct. Mater.*, 2014, **24**, 6172.
36 M. Svensson, F. Zhang, O. Inganäs and M. R. Andersson, *Synth. Met.*, 2003, **135–136**, 137.
37 S. Jungermann, N. Riegel, D. Müller, K. Meerholz and O. Nuyken, *Macromolecules*, 2006, **39**, 8911.
38 A. Charas, H. Alves, J. M. Martinho, L. Alcácer, O. Fenwick, F. Cacialli and J. Morgado, *Synth. Met.*, 2008, **158**, 643.
39 M. C. Gather, A. Köhnen, A. Falcou, H. Becker and K. Meerholz, *Adv. Funct. Mater.*, 2007, **17**, 191.
40 X.-Q. Chen, X. Yao, X. Xiang, L. Liang, W. Shao, F.-G. Zhao, Z. Lu, W. Wang, J. Li and W.-S. Li, *J. Mater. Chem. A*, 2016, **4**, 9286.
41 W. R. Mateker, I. T. Sachs-Quintana, G. F. Burkhard, R. Cheacharoen and M. D. McGehee, *Chem. Mater.*, 2015, **27**, 404.
42 C. Schwarz, H. Bässler, I. Bauer, J.-M. Koenen, E. Preis, U. Scherf and A. Köhler, *Adv. Mater.*, 2012, **24**, 922.